JOURNAL OF AGRICULTURAL AND FOOD CHEMISTRY

Article

pubs.acs.org/JAFC

Mechanistic Insights of Curcumin Interactions with the Core-Recognition Motif of β-Amyloid Peptide

Priyadharshini Kumaraswamy, Swaminathan Sethuraman, and Uma Maheswari Krishnan*

Centre for Nanotechnology & Advanced Biomaterials, School of Chemical & Biotechnology, SASTRA University, Thanjavur 613 401, India

ABSTRACT: Alzheimer's disease is a neurodegenerative disease affecting millions of people worldwide. The proteolytic cleavage of amyloid precursor protein forms amyloid beta peptide ($A\beta_{1-42}$), which aggregates to form senile plaques. The KLVFF motif present in $A\beta_{1-42}$ is essential for aggregation. Curcumin, a prinicipal curcuminoid present in turmeric, shows therapeutic activity against Alzheimer's disease. However, the nature of interaction between the $A\beta_{1-42}$ peptide and curcumin remains unexplored. Studies on the interaction of the core-recognition motif KLVFF with curcumin can be extrapolated to decipher the interactions between $A\beta_{1-42}$ and curcumin. Our data show that curcumin and KLVFF interact strongly through hydrophobic forces and are stabilized by hydrogen bonding. The hydrophobic interactions were confirmed from the positive shift in the phase transition temperature. Fluorescence quenching studies demonstrate a static quenching mechanism. FTIR data confirm the β sheet breaking ability of curcumin, which is also substantiated by cell culture studies.

KEYWORDS: *curcumin, binding affinity, hydrophobic interactions, quenching mechanism, β sheet breaker, Alzheimer's disease*

INTRODUCTION

Curcumin, or 1,7-bis(4-hydroxy-3-methoxyphenyl)-1,6-heptadiene-3,5-dione, the principal curcuminoid of the perennial herb *Curcuma longa* Linn., is a widely used food additive (coloring agent) and spice for many centuries in the Asian subcontinent. In recent years, it has elicited worldwide attention for its therapeutic properties.[1] Curcumin has been extensively investigated for its antioxidant,[2] anti-inflammatory,[3] hypoglycemic,[4] wound-healing,[5] and antimicrobial[6] properties along with its ability to modulate various cell signaling pathways.[7] All properties, namely, physical, chemical, and biological, may be attributed to the unique chemical structure of curcumin and its existence in two tautomeric forms, namely, the keto and enol form (Figure 1a and b).[8] The enol form exhibits better activity because of its ability to accept and donate hydrogen bonds and its ability to chelate positively charged metal ions.[9] The keto−enol tautomerism also allows curcumin to act as a Micheal acceptor to nucleophilic attack, thus enabling them to participate in covalent bond formation.[10]

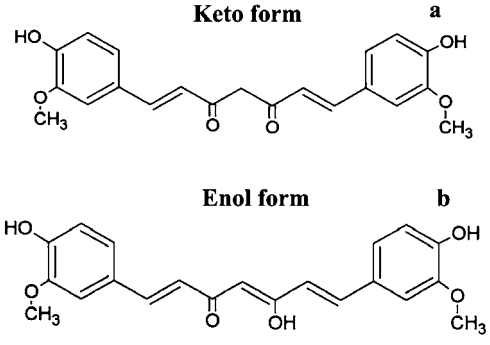

Figure 1. Chemical structures of curcumin: (a) keto form; (b) enol form.

Curcumin consists of an O-methoxy phenolic group on both ends connected by an α,β-unsaturated-β-diketone linker. The aromatic groups and the tautomeric structure are known to influence the hydrophobicity of curcumin, while the linker offers flexibility to the molecule.

Due to its unique structure and property, curcumin is known to bind to a variety of biomolecules such as DNA, RNA, proteins, enzymes, and carrier molecules, thus making curcumin a pharmacologically active molecule.[11,12] One of the major limitations in using curcumin for therapeutic application is its poor bioavailability and stability. However, it is also shown that interaction of curcumin with proteins partly enhances its bioavailability and stability.[13] The interactions between curcumin and various proteins have been widely investigated.[14] The aromatic phenyl groups in curcumin have been known to interact with the aromatic amino acid side chains of the proteins via van der Waals forces and $\pi-\pi$ stacking interactions.[15] Moreover the presence of phenolic and carbonyl functional groups enables it to participate in hydrogen-bonding interactions with the peptide bond of proteins.[16] Apart from the secondary interactions, the keto−enol tautomerism imparts metal chelation ability and covalent bonding character to curcumin, thus providing it an additional functionality.[17]

In recent years, curcumin has been found to be promising in the treatment of Alzheimer's disease. Many reports exist for amyloid β sheet breaking ability of curcumin along with its antioxidant and anti-inflammatory properties for the treatment of Alzheimer's disease.[18] A pilot study was carried out using curcumin and the Chinese herb *Ginkgo bilabo* for the treatment of Alzheimer's disease.[19] Fluorescence studies with thioflavin

Received: January 8, 2013
Revised: March 8, 2013
Accepted: March 12, 2013
Published: March 12, 2013

and scanning electron microscopic studies have revealed the ability of curcumin to destabilize the fibrillar form of both $A\beta_{1-40}$ and $A\beta_{1-42}$.[20] Derivatives of curcumin, namely, isoxazoles and pyrazoles, have been shown to bind Aβ peptide and also inhibit the metabolism of amyloid precursor protein.[21] Moreover, it is also proved by multiphoton microscopy that curcumin has the ability to cross the blood brain barrier[22] and also increases the phagocytosis of Aβ peptide.[23] However, to date there is no study to correlate the mode of interaction of curcumin with the core-recognition motif (KLVFF) of $A\beta_{1-42}$ and its functional activity. Zhao et al. showed using *in silico* molecular dynamic simulations that the hydrophobic interaction and hydrogen-bonding interactions play a vital role in the β sheet breaking ability of curcumin.[24] However, experimental evidence to unravel the nuances involved in the curcumin−amyloid beta interactions is still lacking.

In silico studies such as molecular docking and molecular dynamic simulations provide information about the binding affinity, probable binding site(s), and the possible mode of interactions of curcumin with selected targets.[25] This in turn necessitates the use of advanced *ab initio* molecular orbital methods to correlate the *in silico* findings. However, in order to gain mechanistic insights, the present work aims to study the interaction between the KLVFF peptide and curcumin using simple spectroscopy techniques such as UV−visible spectroscopy and fluorescence spectroscopy, both of which are widely used techniques to understand protein−ligand interactions. The interactions were further confirmed using FT-IR and DSC studies. The correlation between the interactions and the quenching mechanism is also discussed extensively for the first time. Curcumin's β sheet breaking ability and its anti-inflammatory activity are also proven experimentally, and the protection of neuronal cell lines from $A\beta_{1-42}$ peptide toxicity was evaluated using an MTS cytotoxicity assay.

EXPERIMENTAL SECTION

Materials and Methods. $H_2N-KLVFF-CONH_2$, a pentapeptide with >95% purity, was purchased from Bioconcept Laboratories Pvt Ltd. (Gurgaon, India). Curcumin from *Curcuma longa* was procured in powder form from Sigma-Aldrich, India. Peptide stock solutions were prepared using double-distilled water, while curcumin stock solutions were made using methanol because of its poor solubility in double-distilled water. However for all the experiments, curcumin was freshly diluted in double-distilled water and was used immediately to avoid degradation. Amyloid beta peptide ($A\beta_{1-42}$) (AnaSpec, Fremont, CA, USA) was dissolved in 1,1,1,3,3,3-hexafluoroisopropanol (HFIP) at a concentration of 1 mg/mL to remove any aggregates. It was then vacuum evaporated and diluted to the desired concentration using sterile double-distilled water freshly before use.

UV−Visible Spectrophotometry. Absorbance measurements for the determination of binding affinity and binding constants were carried out using a UV−visible spectrophotometer (Lambda 25, Perkin-Elmer, USA) at room temperature. Absorbance titrations were performed using 1 cm quartz cuvettes with the concentration of curcumin (1 or 15 μM) as constant and by the successive additions of increasing concentrations of peptide (7.5 to 30 μM or 10 to 30 μM). The respective spectra were recorded over the wavelength range of 200−800 nm. The concentrations of curcumin (1 and 15 μM) were used based on the therapeutic and toxic concentrations reported.[26] The maximum absorbance values for all concentrations of curcumin and peptide employed in this study were below 1.

Spectrofluorimetry. Fluorescence quenching studies were carried out using a spectrofluorimeter (LS 45, Perkin-Elmer, USA) at room temperature with the bandwidths of both excitation and emission slits at 10 nm. Fluorescence titrations were performed keeping the concentration of peptide (25 μM) constant, and then curcumin was added successively from 1 to 15 μM. The excitation wavelength of peptide was fixed at 257 nm, and emission scans were recorded between 280 and 310 nm. Inner filter effects were corrected by performing the above experiments using UV−visible spectroscopy under similar conditions. The absorbance values at excitation (257 nm) and emission maxima (290 nm) of the peptide were recorded and substituted in the following equation to minimize errors that occur through the inner filter effect.

$$F_{corr} = F_{obs}\ \text{antilog}\left[\frac{(OD_{ex} + OD_{em})}{2}\right]$$

where F_{corr} is the corrected emission intensity, F_{obs} is the observed emission intensity, OD_{ex} is the absorbance value at the excitation wavelength of the peptide, and OD_{em} is the absorbance value at the emission wavelength of the peptide.

Differential Scanning Calorimetry. The interaction between the peptide and curcumin was further confirmed by encapsulating them in liposomes, and thermal analysis was performed for the samples. The liposomes were prepared from egg phosphatidyl choline (Avanti Polar Lipids, Canada) by the thin film hydration technique.[27] The peptide and/or curcumin were loaded into the liposomes using passive loading technique. The size of the liposomes was in the range 150−200 nm. Five mg of liposomal samples were loaded in an aluminum pan along with the reference in a differential scanning calorimeter (DCS; Q20, TA Instruments, USA). The DSC thermogram was recorded between 10 and 180 °C in nitrogen atmosphere at a scan rate of 10 °C/min.

Fourier Transform Infrared Spectroscopy (FT-IR). β sheet breaking ability of the curcumin was confirmed using FT-IR studies. The desired concentration of peptide, namely, 25 μM, was incubated with different concentrations of curcumin, namely, 1, 5, and 10 μM, and FT-IR studies were performed in attenuated total reflectance (ATR) mode using a Fourier transform infrared spectrometer (Spectrum 100, Perkin-Elmer, USA). The analysis was performed between 4000 and 450 cm^{-1} at a resolution of 4 cm^{-1} with 75 average scans per sample.

Cell Culture and Seeding. IMR 32 human neuroblastoma cells procured from National Centre for Cell Sciences (NCCS), Pune, India, were cultured in Dulbecco's modified Eagle medium (DMEM, Gibco, USA) supplemented with 10% fetal bovine serum (FBS, Gibco, USA) and 1% penicillin/streptomycin (Gibco, USA). The culture was maintained at 37 °C in a 5% carbon dioxide incubator. Ten thousand cells were seeded in a 96-well plate and then incubated with 10 μM amyloid beta peptide ($A\beta_{1-42}$) solution for 24 h. After 24 h of incubation, different concentrations of curcumin (1, 2, and 5 μM) were added and incubated again for 48 h.

Cell cytotoxicity was quantified using the 3-(4,5-dimethylthiazol-2-yl)-5-(3-carboxymethoxyphenyl)-2-(4-sulfophenyl)-2*H*-tetrazolium (MTS) assay (Cell Titer 96 AQueous One solution, Promega, USA). After 48 h of incubation with various concentrations of curcumin, the media was removed and the cells were washed with phosphate-buffered saline (PBS) to remove any nonadherent cells. Then 200 μL of serum-free media and 20 μL of MTS reagent were added and incubated at 37 °C for 2 h. The reaction was stopped by the addition of 25 μL of 10% sodium dodecyl sulfate (SDS) solution. The absorbance was then measured at 490 nm using a multimode reader (Infinite 200M, Tecan, USA). Cells incubated with 10 μM amyloid beta peptide ($A\beta_{1-42}$) served as a positive control, while cells without amyloid beta peptide ($A\beta_{1-42}$) served as a negative control.

Interleukin 12 (IL-12) Assay. Concentration of the inflammatory cytokine IL-12 in the cell supernatant was evaluated using the IL-12 ELISA kit procured from R & D Systems, USA. After 24 h of incubation in different concentrations of curcumin added to the IMR-32 neuroblastoma cell lines incubated with $A\beta_{1-42}$, the supernatant was collected and the IL-12 assay was performed in duplicates according to the manufacturer's protocol. After completion of the assay procedure, absorbance was recorded at 450 nm using a multimode reader (Infinite 200M, Tecan, USA). For blank correction, absorbance was recorded at 540 nm and the actual values were subtracted from it. The concentration of IL-12 in the positive and negative controls along

dx.doi.org/10.1021/jf4000709 | J. Agric. Food Chem. 2013, 61, 3278−3285

with various curcumin-treated samples was calculated using the standard graph.

Statistical Analysis. Analysis of variance (one-way ANOVA) was performed to determine the statistical significance ($p < 0.05$) for MTS ($n = 3$) and IL-12 assays.

RESULTS AND DISCUSSION

UV−Visible Studies. Curcumin consists of a 1,3-diketone moiety that enables an extended conjugation of the π electron system between the two feruloyl groups. Because of the 1,3-diketone moiety, curcumin can exist in an equilibrium mixture of two possible tautomeric forms, namely, the keto and enol form (Figure 1). The existence of a conjugated network of the π electron system between the two feruloyl groups makes the enol form more stable in solid and solution state.[28] It also has the ability to chelate metal ions and scavenge free radicals.

An aqueous methanolic curcumin solution showed absorption maxima of 421 nm with a shoulder at 360 nm and a weak absorption band around 260 nm (Figure 2). The extensive

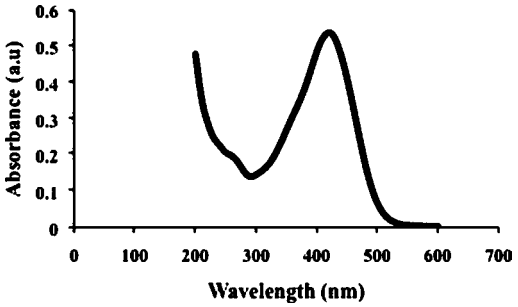

Figure 2. Absorption spectrum of an aqueous methanolic solution of curcumin.

delocalization of π electrons throughout the molecule between the feruloyl groups lowers the $\pi^* \leftarrow \pi$ transition energy, resulting in a peak at 421 nm, confirming the presence of the enolic form of curcumin.[29] Lack of a peak at 389 nm indicates the absence of the keto form of curcumin.

Figure 3a shows the absorption spectra for 15 μM curcumin in the absence and presence of different concentrations of KLVFF peptide (7.5−30 μM). The absorption spectrum of curcumin exhibits a prominent peak at 421 nm and a weak absorption band at 257 nm. A weak shoulder at 360 nm is also observed. These peaks arise due to the $\pi^* \leftarrow$ n and $\pi^* \leftarrow \pi$ transitions in curcumin. The forbidden $\pi^* \leftarrow$ n transition occurs in the high-energy ultraviolet region of the spectrum (257 nm), while the $\pi^* \leftarrow \pi$ transitions occur in the lower energy end of the spectrum (357 and 421 nm). The intensity and position of the absorption bands occurring due to the $\pi^* \leftarrow \pi$ electronic transitions are influenced by many parameters. These include dipole−dipole interactions, intermolecular and intramolecular hydrogen bonding, temperature, and hydrophilicity of the environment. These interactions, if present in the system, can alter the absorption and emission spectrum of curcumin. The intensity of the absorption bands at 421 and 257 nm gradually decreases on successive addition of peptide, and isosbestic points were observed at 227 and 492 nm. However, the shoulder at 360 nm becomes more pronounced. The formation of an isosbestic point confirms the existence of interactions between curcumin and KLVFF peptide, and both interacting species exist in equilibrium with one another at that particular wavelength. The intensity of the band at 421 nm is indicative of a greater hydrophobic/nonpolar environment,[30] while the shoulder at 360 nm implies a more polar environment. Addition of peptide increases the polarity due to its charged nature, which also may be the reason for the decreased intensity at 421 nm.

When a minimum concentration of curcumin (1 μM) was used, a sharp peak at 421 nm, a shoulder at 360 nm, and a weak absorption band at 257 nm are visible in the absorption spectrum (Figure 3c). When the peptide concentration is increased from 10 μM to 30 μM, the absorption at 421 and 360 nm decreases, while the absorption at 257 nm increases. This increase may be ascribed to the presence of the peptide whose absorption maximum is around 260 nm. The isosbestic points occur at 388 and 470 nm, suggesting the existence of interactions between the peptide and curcumin. However, the mode of interaction might be dependent on the concentration of curcumin, as evidenced from the different isosbestic points obtained in both cases. When a maximum concentration of curcumin (15 μM) is used, a bathochromic shift in the absorption maxima from 421 nm to 425 nm is observed. Such bathochromic shifts are generally ascribed to the intermolecular interactions.[31] As the peptide molecule contains both hydrogen bond donors and acceptors, the bathochromic shift observed on the addition of peptide indicates the possibility of hydrogen bond formation between the KLVFF peptide and curcumin. On the other hand, there is no shift observed in the minimum concentration of curcumin. However, in both cases, the pattern of the absorption spectra is not altered, indicating that the central diketone moiety and the conjugated π electron system between the feruloyl groups are not perturbed. The decrease in absorbance at 421 nm in the case of the maximum concentration of curcumin (15 μM) and 421 and 360 nm peaks in the case of the minimum concentration of curcumin (1 μM) may be attributed to the involvement of feruloyl groups. Since these groups resemble the structure of phenylalanine present in the KLVFF peptide, they may associate via hydrophobic interactions ($\pi-\pi$, van der Waals). Figure 4 shows the schematic representation of the different modes of interaction between KLVFF peptide and curcumin.

Let us consider the following equilibrium:

$$\text{curcumin} + \text{peptide} \rightleftharpoons \text{curcumin–peptide}$$

The association constant (K_a) can be calculated from the following equation:

$$\frac{1}{\Delta A} = \frac{1}{(\varepsilon_b - \varepsilon_f)L_T} + \frac{1}{(\varepsilon_b - \varepsilon_f)L_T K_a}\frac{1}{M}$$

where ε is the molar extinction coefficient and the subscripts b, f, and T refers to the bound, free, and total ligand concentration; L refers to the ligand (curcumin, 1 or 15 μM), and M refers to the macromolecule (peptide, 7.5 to 30 μM or 10 to 30 μM). The equilibrium constant can be calculated by measuring the absorbance at a fixed wavelength. A double-reciprocal plot is obtained by plotting $1/(A_0 - A)$ against 1/[peptide] (Figure 3b and d). The ratio of intercept and the slope gives the K_a value, which is found to be 1.131×10^5 M^{-1} for 15 μM curcumin concentration and 3.786×10^4 M^{-1} for 1 μM curcumin concentration. These values are well in agreement with the K_a values reported for strong interactions.[32] The absorbance value decreases by 25% and 20% for 15 and 1 μM curcumin concentration, respectively. There is not much difference observed when two different concentrations of curcumin were used. A similar trend was observed in the K_a

dx.doi.org/10.1021/jf4000709 | J. Agric. Food Chem. 2013, 61, 3278−3285

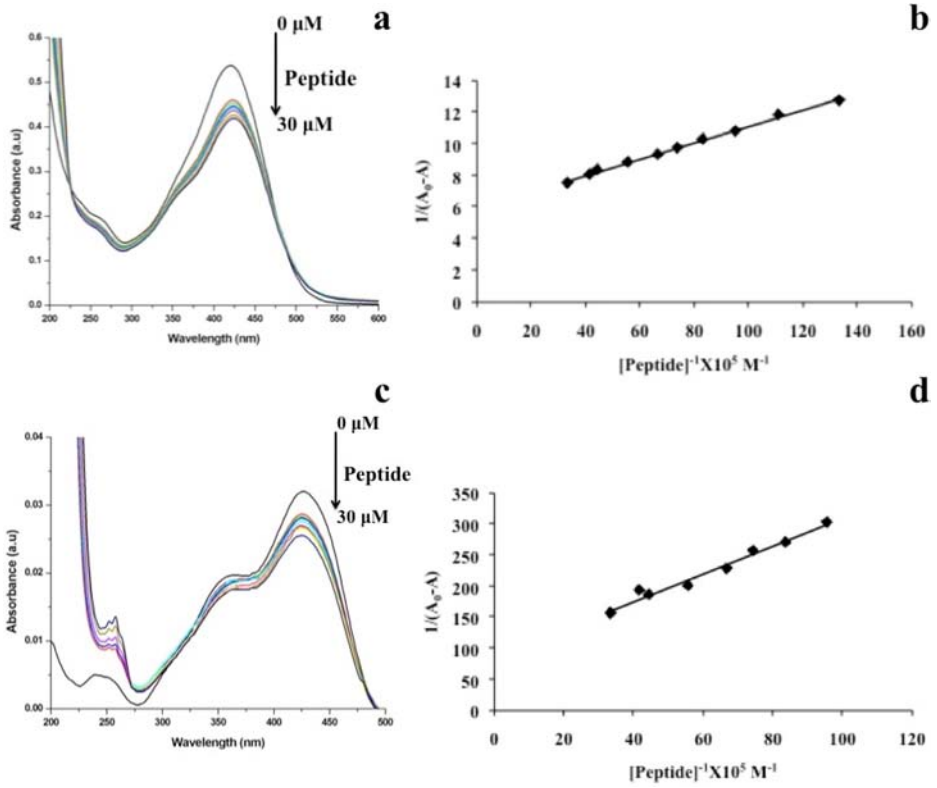

Figure 3. (a) UV−visible spectral changes of curcumin (15 μM) in the absence and presence of KLVFF peptide (7.5−30 μM). (b) Double-reciprocal plot for 15 μM curcumin and 7.5−30 μM peptide. (c) UV−visible spectral changes of curcumin (1 μM) in the absence and presence of KLVFF peptide (10−30 μM). (d) Double-reciprocal plot for 1 μM curcumin and 10−30 μM peptide.

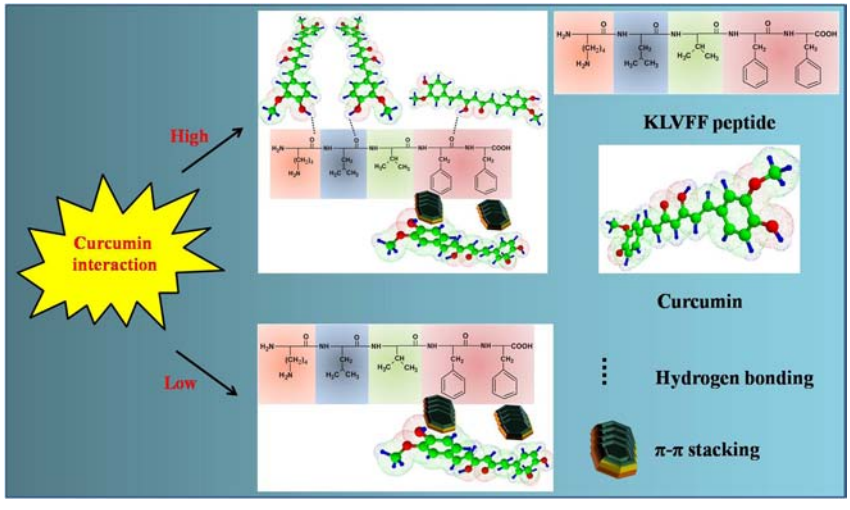

Figure 4. Schematic representation of interaction between KLVFF peptide and curcumin: hydrogen bonding and hydrophobic interactions.

values, whose binding affinity was unaltered due to changes in curcumin concentration. From the above experiments it becomes evident, for efficient binding with KLVFF, more than 1 μM and less than 15 μM concentration of curcumin is required. This is in agreement with the therapeutic levels of curcumin required for disruption of amyloid plaque.[26]

Fluorescence Quenching Studies. Due to the aromatic phenylalanine residues present in the peptide sequence KLVFF, the emission peak was observed at 290 nm, when excited at 257 nm. For quenching studies, two different concentrations of the peptide corresponding to the maximum and minimum absorbance value (25 and 1 μM) were chosen. From the literature studies, it is obvious that aggregation of amyloid beta peptide happens only at micromolar concentrations.[33] Moreover, it is known from the previous reports that 10 μM amyloid beta peptide is sufficient to reduce the cell count to half.[34] Figure 5a shows the quenching of KLVFF peptide fluorescence by curcumin between 1 and 15 μM. It was observed that successive addition of different concentrations of curcumin (1−15 μM) reduced the fluorescence intensity of the peptide without any spectral shift. This clearly shows that the quenching of the intrinsic fluorescence of the peptide is due to the association of the peptide and curcumin through attractive forces. Quenching is quantitatively determined using

dx.doi.org/10.1021/jf4000709 | J. Agric. Food Chem. 2013, 61, 3278−3285

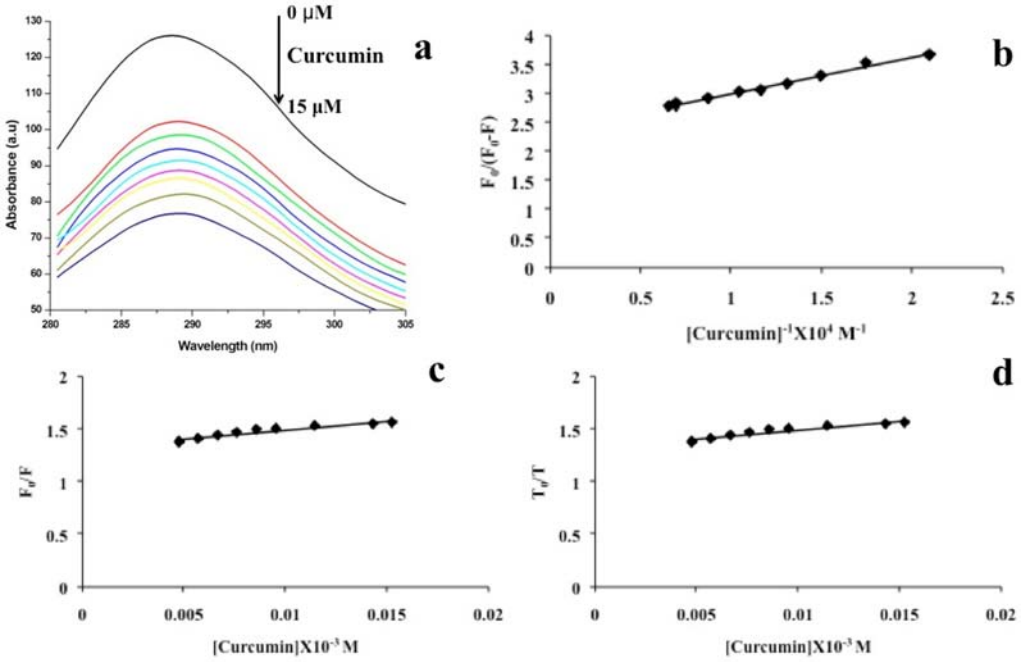

Figure 5. (a) Fluorescence emission spectrum of KLVFF peptide (25 μM) in the presence of curcumin (1−15 μM), λ_{ex} = 257 nm and λ_{em} = 290 nm. (b) Modified Stern−Volmer plot. (c) Stern−Volmer plot of fluorescence emission intensity. (d) Stern−Volmer plot of fluorescence lifetime.

a modified Stern−Volmer plot, which helps to calculate the quenching constant K_a and the number of fluorophores accessible to the ligand.

$$\frac{F_0}{(F_0 - F)} = \frac{1}{f_a K_a}\frac{1}{Q} + \frac{1}{f_a}$$

In the above equation, F_0 denotes the fluorescence intensity in the absence of quencher (curcumin) and F denotes the fluorescence intensity in the presence of quencher; f_a and K_a denote the fraction of accessible fluorophore and quenching constant, respectively. Based on the modified Stern−Volmer equation, a plot of $F_0/(F_0 - F)$ was made against 1/[curcumin] (Figure 5b). The quenching constant K_a was calculated from the ratio of the intercept to the slope, and the fraction of accessible fluorophore (f_a) was calculated from the inverse of the intercept, which were found to be 3.756 × 10^5 M^{-1} and 0.423, respectively.

Quenching can also be analyzed using the Stern−Volmer quenching constant K_{SV} using the equation

$$\frac{F_0}{F} = 1 + K_{SV}[Q] = 1 + k_q\tau_0[Q]$$

The plot of F_0/F against the concentration of curcumin (Figure 5c) helps to find the Stern−Volmer quenching constant K_{SV}, which was found to be 1.689 × 10^4 M^{-1}. Quenching can be either static or dynamic. Static quenching occurs when there is complex formation between the fluorophore and the quencher in the ground state, due to which the number of fluorophores residing in the excited state was reduced. Hence, the emission intensity of the fluorophore decreases in the presence of quencher. Dynamic or collision quenching occurs when the interaction between the fluorophore and quencher takes place in the excited state. The main difference between the static and dynamic quenching lies in the lifetime of the fluorescence (10^{-8} s) for various concentrations of the quencher, which is not altered in static quenching (interaction happens only in the ground state). On the other hand, the diffusion and random collision of the quencher with the fluorophore in the excited state take place in dynamic quenching. Hence the lifetime of the fluorescence is reduced as the concentration of the quencher increases.

Initially a dynamic quenching model was assumed between KLVFF and curcumin. For dynamic quenching, the following relation can be used:

$$K_{SV} = K_q T_0$$

where K_{SV} is the Stern−Volmer quenching constant, K_q is the bimolecular quenching constant, and T_0 is the lifetime of fluorescence (10^{-8} s). K_{SV} was found to be 1.689 × 10^4 M^{-1}, and K_q is 1.689 × 10^{12} M^{-1} s^{-1}, which is greater than the largest bimolecular quenching constant (10^{10} M^{-1} s^{-1}) in aqueous medium. From the above value it is clear that the quenching is not due to collision factors but rather due to the association between the fluorophore and quencher in the ground state.

The plot of T_0/T versus concentration of curcumin also exhibits linearity, suggesting that the fluorescence lifetime is not altered even when the concentration of curcumin is increased, confirming the static quenching phenomenon occurring in the system on addition of curcumin (Figure 5d). The interactions between KLVFF and curcumin can be favored by the aromatic $\pi-\pi$ stacking associations involving the feruloyl moieties of curcumin and the phenylalanine residues of KLVFF. The planarity of the curcumin facilitates such stacking interactions. In addition, intermolecular hydrogen bonding may also exist between the two molecules, and as a result, static quenching was observed in the system. A similar mode of interaction between curcumin and peptide was in good agreement with the results of the binding studies, which show there exists a close association between the feruloyl groups of the curcumin and the phenylalanine residue of the KLVFF peptide.

Thermal Analysis. In order to further ascertain the nature of interactions between KLVFF peptide and curcumin, both the

dx.doi.org/10.1021/jf4000709 | J. Agric. Food Chem. 2013, 61, 3278−3285

peptide and curcumin were encapsulated in liposomes individually as well as together and subjected to thermal analysis. Figure 6 shows the phase transition temperature of

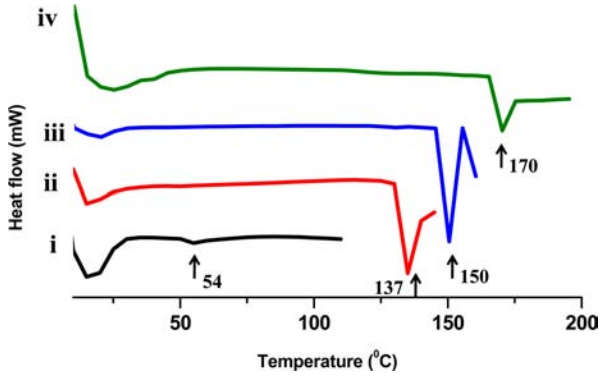

Figure 6. Differential scanning calorimetry (DSC) thermograms of blank, peptide-loaded, curcumin-loaded, and dual-loaded liposomes.

plain liposomes and loaded liposomes. The gel to liquid crystalline phase transition temperature of the plain liposome was 54 °C, and that of the peptide-loaded liposome was 137 °C. Curcumin-loaded liposomes exhibit a phase transition temperature of 150 °C, while that for the dual-loaded liposome occurred at 170 °C. In all three cases (peptide loaded, curcumin loaded, and dual molecule loaded), the T_m is shifted to higher temperature compared to the plain liposome, indicating that they are located in the hydrophobic core of the liposome, resulting in rigidification of the liposomal membrane. Interestingly, the dual-loaded liposome exhibits a single peak instead of two peaks expected for peptide and curcumin, indicating no phase separation due to the incorporation of these two molecules in the lipid bilayer. These results suggest the existence of interaction between KLVFF and curcumin, which is most likely to be hydrophobic.

FTIR Studies. The mechanism by which curcumin disrupts the amyloid plaques is poorly understood. From the binding and fluorescence studies, it was observed that $\pi-\pi$ hydrophobic interactions between the feruloyl group of the curcumin and phenylalanine residues of the KLVFF peptide exist. Figure 7 shows the FTIR spectra of peptide (25 μM) and various

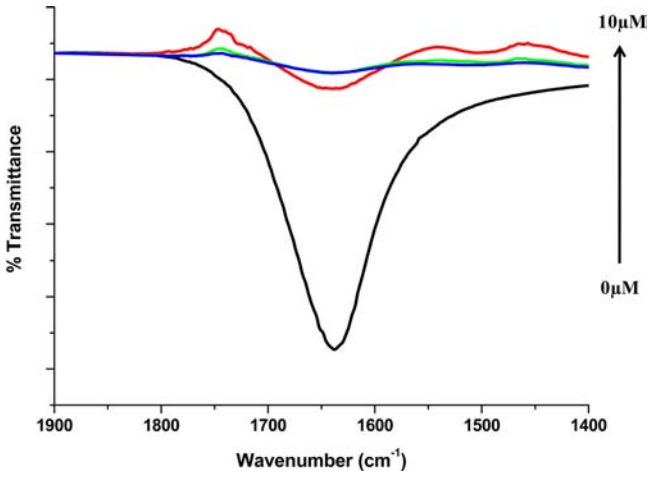

Figure 7. FT-IR spectra of peptide (25 μM) with various concentrations of curcumin (1, 5, and 10 μM).

concentrations of curcumin (1, 5, 10 μM) incubated with 25 μM peptide. In the absence of curcumin, the peptide exhibits a band at 1638 cm^{-1} that is attributed to hydrogen-bonded β sheet structures.[35] On addition of increasing concentrations of curcumin, the intensity at 1638 cm^{-1} decreases drastically, which is an indication of disruption of hydrogen-bonded β sheet structures by curcumin. These results offer strong experimental evidence in support of the molecular dynamics simulation studies reported, which had suggested that curcumin disrupts the amyloid aggregates probably due to stacking interactions with the aromatic residues in the amyloid beta peptide.[24]

IL-12 Assay. IL-12 is a heterodimeric cytokine produced by dendritic cells in response to an antigen. It is already established that the secretion of pro-inflammatory cytokines such as TNF-α and IL-12 is induced in response to amyloid beta in peripheral monocyte culture.[36] Moreover, treatment of microglial cells with either lipopolysaccharide or amyloid beta induces the expression of m-RNA levels of TNF-α and IL-12.[37] When amyloid beta peptide aggregates to form plaques, microglial cells will be activated, which try to phagocytose the aggregates. The activation of microglial cells results in the enhanced secretion of inflammatory cytokines such as IL-12. Thus IL-12 is an important biomarker, and it is significantly associated with Alzheimer's disease. Therefore any disruption in the aggregation of amyloid beta peptide will result in reduction in IL-12 levels. However, no reports exist so far in IMR-32 human neuroblastoma cell lines. Moreover, the spectroscopic studies have also indicated that curcumin interacts with the KLVFF peptide, resulting in the disruption of β sheet structures, and hence an attempt has been made to determine the influence of curcumin on IL-12 levels in cells incubated with $A\beta_{1-42}$.

Figure 8a shows the influence of curcumin on the IL-12 levels in neuroblastoma cells. IMR-32 human neuroblastoma cells incubated with $A\beta_{1-42}$ for 48 h served as a positive control, while untreated cells served as a negative control. The presence of amyloid beta peptide increased the pro-inflammatory IL-12 cytokine level significantly when compared to the negative control. After $A\beta_{1-42}$ incubation, the cells were treated with different concentrations of curcumin (1, 2, 5 μM) for 24 h. After 24 h, it was observed that the IL-12 levels were significantly lowered in cells treated with 2 and 5 μM curcumin. The decrease in IL-12 levels by curcumin may be due to the anti-inflammatory nature of curcumin[38] or may be due to the interaction of curcumin with amyloid beta peptide, which prevents the $A\beta_{1-42}$ from stimulating IL-12 production. Correlating with the observations from Figure 3, it is likely that in Alzheimer-related conditions the curcumin–$A\beta_{1-42}$ interactions might contribute to the lowering of IL-12 levels, thereby increasing cell viability.

Cell Viability Assay. Further confirmation on the ability of curcumin to disrupt the β sheet structures formed by amyloid beta peptide was obtained from cell viability studies using IMR-32 human neuroblastoma cells. Figure 8b shows the results obtained from an MTS assay with curcumin-treated and untreated cells. Treatment of cells using 10 μM $A\beta_{1-42}$ decreases cell viability to half. However, when curcumin is added (1, 2, and 5 μM), the viability is enhanced, and the results show that even 2 μM curcumin concentration is enough to overcome the cytotoxicity caused by $A\beta_{1-42}$. The maximum concentration of curcumin used in the study was maintained at 5 μM since at higher concentrations it has been reported to be

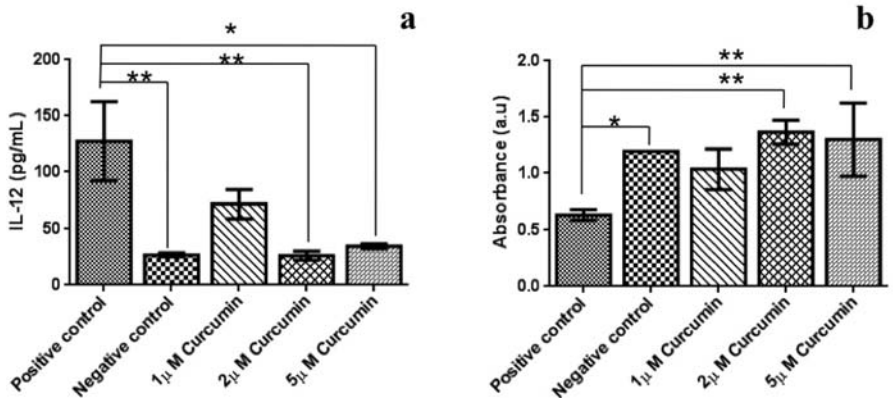

Figure 8. (a) IL-12 assay for various concentrations of curcumin in IMR-32 neuroblastoma cell lines incubated with $A\beta_{1-42}$ peptide. (b) Cell cytotoxicity assay for various concentrations of curcumin in IMR-32 neuroblastoma cell lines incubated with $A\beta_{1-42}$ peptide (*,**$p < 0.05$).

cytotoxic.[26] These amyloid beta aggregates are known to induce free radical production and microglial activation, thus causing cytotoxicity. Since curcumin acts as a free radical scavenger and an anti-inflammatory agent, it can overcome the cytotoxicity caused by $A\beta_{1-42}$ aggregates. Another reason may be its ability to disrupt the amyloid beta aggregates by interacting with them via hydrophobic interactions. Cell cytotoxicity results were in agreement with the FT-IR results, which show that the presence of curcumin destabilizes the β sheet structure adopted by the KLVFF motif in amyloid beta peptide.

Thus this work summarizes the interaction studies of KLVFF and curcumin carried out using UV−visible spectrophotometry, fluorescence spectroscopy, differential scanning calorimetry, and FT-IR spectroscopy. Binding constants on the order of 10^4−10^5 show there exists a strong binding affinity between KLVFF peptide and curcumin. UV−visible spectroscopy further confirmed the absence of involvement of the central diketone moiety and the involvement of feruloyl groups, which in turn are responsible for the secondary interactions. The results suggest the existence of hydrogen-bonding interactions between KLVFF peptide and curcumin at certain concentrations. However, it is more likely that the hydrophobic interactions between the phenylalanine moiety of KLVFF and the feruloyl groups of curcumin are responsible for stabilizing the interactions. Fluorescence quenching experiments prove that the mechanism of fluorescence quenching by curcumin follows static quenching, which may also be attributed to the secondary interactions (hydrogen-bonding interactions and hydrophobic interactions) that exist between the two molecules. The β sheet breaking ability of curcumin, as shown by FT-IR studies and cell viability data, can also be attributed to the interactions that exist between curcumin and KLVFF peptide. The peptide−curcumin interactions may also stabilize curcumin in an aqueous environment, thus enhancing the therapeutic index of this molecule to treat Alzheimer's disease.

AUTHOR INFORMATION

Corresponding Author

*Phone: (+91) 4362 264101, ext. 3677. Fax: (+91) 4362 264120. E-mail: umakrishnan@sastra.edu.

Notes

The authors declare no competing financial interest.

ACKNOWLEDGMENTS

The authors wish to acknowledge SASTRA University and PG Teaching Programme (No. SR/NM/PG-16/2007) of the Nano Mission Council, Department of Science & Technology, New Delhi, for the infrastructural support. The first author (P.K) also wishes to thank the Department of Science & Technology for the INSPIRE Fellowship grant (DST/INSPIRE Fellowship/2011/74).

REFERENCES

(1) Hatcher, H.; Planalp, R.; Cho, J.; Torti, F. M.; Torti, S. V. Curcumin: from ancient medicine to current clinical trials. *Cell. Mol. Life. Sci.* **2008**, *65*, 1631−1652.

(2) Sharma, O. P. Antioxidant activity of curcumin and related compounds. *Biochem. Pharmacol.* **1976**, *25* (15), 1811−1812.

(3) Gupta, S. C.; Kim, J. H.; Prasad, S.; Aggarwal, B. B. Regulation of survival, proliferation, invasion, angiogenesis, and metastasis of tumor cells through modulation of inflammatory pathways by nutraceuticals. *Cancer Metastasis Rev.* **2010**, *29* (3), 405−434.

(4) Sharma, S.; Kulkarni, S. K.; Chopra, K. Curcumin, the active principle of turmeric (*Curcuma longa*), ameliorates diabetic nephropathy in rats. *Clin. Exp. Pharmacol. Physiol.* **2006**, *33* (10), 940−945.

(5) Sidhu, G. S.; Singh, A. K.; Thaloor, D.; Banaudha, K. K.; Patnaik, G. K.; Srimal, R. C.; Maheswari, R. K. Enhancement of wound healing by curcumin in animals. *Wound Repair Regen.* **1998**, *6* (2), 167−177.

(6) Negi, P. S.; Jayaprakasha, G. K.; Jagan Mohan Rao, L.; Sakariah, K. K. Antibacterial activity of turmeric oil: a byproduct from curcumin manufacture. *J. Agric. Food Chem.* **1999**, *47* (10), 4297−4300.

(7) Gupta, S. C.; Prasad, S.; Kim, J. H.; Patchva, S.; Webb, L. J.; Priyadarsini, I. K.; Aggarwal, B. B. Multitargeting by curcumin as revealed by molecular interaction studies. *Nat. Prod. Rep.* **2011**, *28*, 1937−1955.

(8) Tonnesen, H. H.; Karlsen, J.; Mostad, A. Structural studies of curcuminoids. I. The crystal structure of curcumin. *Acta Chem. Scand. B* **1982**, *36*, 475−479.

(9) Borsari, M.; Ferrari, E.; Grandi, R.; Saladini, M. Curcuminoids as potential new iron-chelating agents: spectroscopic, polarographic and potentiometric study on their Fe (III) complexing ability. *Inorg. Chem. Acta* **2002**, *328*, 61−68.

(10) Fang, J.; Lu, J.; Holmgren, A. Thiredoxin reductase is irreversibly modified by curcumin: a novel molecular mechanism for its anticancer activity. *J. Biol. Chem.* **2005**, *280* (26), 25284−25290.

(11) Bera, R.; Sahoo, B. K.; Ghosh, K. S.; Dasgupta, S. Studies on the interaction of isoxazolcurcumin with calf thymus DNA. *Int. J. Biol. Macromol.* **2008**, *42* (1), 14−21.

(12) Kunnumakkara, A. B.; Anand, P.; Aggarwal, B. B. Curcumin inhibits proliferation, invasion, angiogenesis and metastasis of different

cancers through interaction with multiple cell signaling proteins. *Cancer Lett.* **2008**, *269* (2), 199−225.
(13) Leung, M. H.; Kee, T. W. Effective stabilization of curcumin by association to plasma proteins: human serum albumin and fibrinogen. *Langmuir* **2009**, *25* (20), 5773−5777.
(14) Wang, F.; Yang, J.; Wu, X.; Liu, S. Study of the interaction of proteins with curcumin and SDS and its analytical application. *Spectrochim. Acta A: Mol. Biomol. Spectrosc.* **2005**, *61* (11−12), 2650−2656.
(15) Sneharani, A. H.; Karakkat, J. V.; Singh, S. A.; Rao, A. G. A. Interaction of curcumin with β-lactoglobulin−Stability, spectroscopic analysis and molecular modeling of the complex. *J. Agric. Food Chem.* **2010**, *58* (20), 11130−11139.
(16) Mohammadi, F.; Bordbar, A. K.; Divsalar, A.; Mohammadi, K.; Saboury, A. A. Interaction of curcumin and diacetylcurcumin with the lipocalin member beta-lactoglobulin. *Protein J.* **2009**, *28* (3−4), 117−123.
(17) Baum, L.; Ng, A. Curcumin interaction with copper and iron suggests one possible mechanism of action in Alzheimer's disease animal models. *J. Alzheimers Dis.* **2004**, *6*, 367−377.
(18) Kim, J.; Lee, H. J.; Lee, K. W. Naturally occurring phytochemicals for the prevention of Alzheimer's disease. *J. Neurochem.* **2009**, *112* (6), 1415−1430.
(19) http://www.clinicaltrials.gov (NCT00164749).
(20) Ono, K.; Hasegawa, K.; Naiki, H.; Yamada, M. J. Curcumin has potent anti-amyloidogenic effects for Alzheimer's beta fibrils *in vitro*. *Neurosci. Res.* **2004**, *75*, 742−750.
(21) Narlawar, R.; Pickhardt, M.; Leuchtenberger, S.; Baumann, K.; Krause, S.; Dyrus, T.; Weggen, S.; Mandelkow, E.; Schmidt, B. Curcumin-derived pyrazoles and isoxazoles: Swiss army knives or blunt tools for Alzheimers disease? *Chem. Med. Chem.* **2008**, *3*, 165−172.
(22) Garcia-Alloza, M.; Borrelli, L. A.; Rozkalne, A.; Hyman, B. T.; Bacskai, B. J. Curcumin labels amyloid pathology in vivo, disrupts existing plaques and partially restores distorted neuritis in an Alzheimer mouse model. *J. Neurochem.* **2007**, *102*, 1095−1104.
(23) Fiala, M.; Liu, P. T.; Espinosa-Jeffrey, A.; Rosenthal, M. J.; Bernard, G.; Ringman, J. M.; Sayre, J.; Zhang, L.; Zaghi, J.; Dejbakhsh, S.; et al. Innate immunity and transcription of MGAT-III and toll-like receptors in Alzheimers disease patients are improved by bisdemethoxycurcumin. *Proc. Natl. Acad. Sci. U.S.A.* **2007**, *104*, 12849−12854.
(24) Zhao, L. N.; Chiu, S.-W.; Benoit, J.; Chew, L. Y.; Mu, Y. The effect of curcumin on the stability of Aβ dimers. *J. Phys. Chem. B* **2012**, *116*, 7428−7435.
(25) Wua, S. T.; Sun, J.-C.; Lee, K.-J.; Sun, Y.-M. Docking prediction for tumor necrosis factor-α and five herbal inhibitors. *Int. J. Eng. Sci. Tech.* **2010**, *2* (9), 4263−4277.
(26) Yang, F.; Lim, G. P.; Begum, A. N.; Ubeda, O. J.; Simmons, M. R.; Ambegaokar, S. S.; Chen, P.; Kayed, R.; Glabe, C. G.; Frautschy, S. A.; Cole, G. M. Curcumin inhibits formation of amyloid β oligomers and fibrils, binds plaques, and reduces amyloid *in vivo*. *J. Biol. Chem.* **2005**, *280* (7), 5892−5901.
(27) Ramana, L. N.; Sethuraman, S.; Ranga, U.; Krishnan, U. M. Development of a liposomal nanodelivery system for nevirapine. *J. Biomed. Sci.* **2010**, *17*, 57−65.
(28) Pedersen, U.; Rasmussen, P. B. Synthesis of naturally occurring curcuminoids and related compounds. *Liebigs Ann. Chem.* **1985**, *8*, 1557−1569.
(29) Christian, G. D.; O'Relly, J. E. *Ultraviolet and Visible Absorption Spectroscopy in Instrumental Analysis*, 2nd ed.; Allyn and Bacon: Boston, 1986; pp 161−207.
(30) Gopinath, D.; Rafiuddin ahmed, M.; Gomathi, K.; Chitra, K.; Sehgal, P. K.; Jayakumar, R. Dermal wound healing processes with curcumin incorporated collagen films. *Biomaterials* **2004**, *25*, 1911−1917.
(31) Vallejo, J. J.; Mesa, M.; Gallardo, C. Evaluation of Avobenzone photostability in solvents used for cosmetic applications. *Vitae* **2011**, *18*, 63−71.
(32) Sahoo, B. K.; Ghosh, K. S.; Dasgupta, S. An investigation of the molecular interactions of diacetylcurcumin with ribonuclease A. *Protein Peptide Lett.* **2009**, *16*, 1485−1495.
(33) Clementi, M. E.; Pezzotti, M.; Orsini, F.; Sampaolese, B.; Mezzogori, D.; Grassi, C.; Giardina, B.; Misiti, F. Alzheimer's amyloid β-peptide (1−42) induces cell death in human neuroblastoma via bax/bcl−2 ratio increase: An intriguing role for methionine 35. *Biochem. Biophys. Res. Commun.* **2006**, *342*, 206−213.
(34) Park, S.-Y.; Kim, H.-S.; Cho, E.-K.; Kwon, B.-Y.; Phark, S.; Hwang, K.-W.; Sul, D. Curcumin protected PC12 cells against beta-amyloid-induced toxicity through the inhibition of oxidative damage and tau hyperphosphorylation. *Food Chem. Toxicol.* **2008**, *46*, 2881−2887.
(35) Kumaraswamy, P.; Lakshmanan, R.; Sethuraman, S.; Krishnan, U. M. Self-assembly of peptides: influence of substrate, pH and medium on the formation of supramolecular assemblies. *Soft Matter* **2011**, *7*, 2744−2754.
(36) Fiala, M.; Zhang, L.; Gan, X.; Sherry, B.; Taub, D.; Graves, M. C.; Hama, S.; Way, D.; Weinand, M.; Witte, M.; Lorton, D.; Kuo, Y. M.; Roher, A. E. Amyloid-beta induces chemokine secretion and monocyte migration across a human blood−brain barrier model. *Mol. Med.* **1998**, *4* (7), 480−489.
(37) Nagai, A.; Nakagawa, E.; Hatori, K.; Choi, H. B.; McLarnon, J. G.; Lee, M. A.; Kim, S. U. Generation and characterization of immortalized human microglial cell lines: expression of cytokines and chemokines. *Neurobiol. Dis.* **2001**, *8* (6), 1057−1068.
(38) Mishra, S.; Palanivelu, K. An effect of curcumin (turmeric) on Alzheimer's disease: an overview. *Ann. Indian Acad. Neurol.* **2008**, *11*, 13−19.